

GNSS radio occultation
constellation observing system
experiments

Peter Bauer, Gábor Radnóti, Sean Healy,
Carla Cardinali

Research Department

Submitted to Monthly Weather Review

February 2013

*This paper has not been published and should be regarded as an Internal Report from ECMWF.
Permission to quote from it should be obtained from the ECMWF.*



Series: ECMWF Technical Memoranda

A full list of ECMWF Publications can be found on our web site under:

<http://www.ecmwf.int/publications/>

Contact: library@ecmwf.int

©Copyright 2013

European Centre for Medium-Range Weather Forecasts
Shinfield Park, Reading, RG2 9AX, England

Literary and scientific copyrights belong to ECMWF and are reserved in all countries. This publication is not to be reprinted or translated in whole or in part without the written permission of the Director-General. Appropriate non-commercial use will normally be granted under the condition that reference is made to ECMWF.

The information within this publication is given in good faith and considered to be true, but ECMWF accepts no liability for error, omission and for loss or damage arising from its use.

Abstract

Observing system experiments within the operational ECMWF data assimilation framework have been performed for summer 2008 when the largest recorded number of GNSS radio occultation observations from both operational and experimental satellites has been available. Constellations with 0, 5, 33, 67, and 100% data volume were assimilated to quantify the sensitivity of analysis and forecast quality to radio occultation data volume. These observations mostly constrain upper tropospheric and stratospheric temperatures and correct an apparent model bias that changes sign across the upper troposphere - lower stratosphere. This correction effect does not saturate with increasing data volume, even if more data is assimilated than available in today's analyses. Another important function of radio occultation data, namely the anchoring of variational radiance bias corrections, is demonstrated in this study. This effect also does not saturate with increasing data volume. In the stratosphere, the anchoring by radio occultation data is stronger than provided by radiosonde and aircraft observations.

sectionIntroduction The feasibility of making radio occultation (RO) measurements using Global Navigation Satellite System transmissions (GNSS-RO) was demonstrated in the GPS/MET [14, 19] and CHAMP [20] missions. GNSS-RO measurements have subsequently proven to be a very valuable addition to the operational numerical weather prediction (NWP) observing system, since the launch of the FORMOSAT-3/COSMIC constellation of receivers in 2006 [1]. The measurements are particularly useful in NWP because they can be assimilated without bias correction, and they have strong sensitivity to upper atmospheric temperature structures, an area that is otherwise only weakly constrained by other observations in the analysis, and that is prone to large model uncertainties. Many operational NWP centres have now reported a significant impact on upper tropospheric and stratospheric temperatures in their NWP systems with the current number of observations [13, 7, 2, 17, 18], and they also have a significant impact in climate reanalyses [15].

To date, only receivers of the Global Positioning System (GPS) signals have been deployed. Hereafter, these will be referred to as GPS-RO observations. In the future, it is expected to also have multiple receivers using the European Galileo and other systems, such as Globalnaya Navigatsionnaya Sputnikovaya Sistema (GLONASS), which will potentially greatly increase the number of occultations available for assimilation into NWP systems. However, it is an open question if more occultation measurements are required for NWP applications, or whether the impact of GPS-RO is already close to saturation with the current observation numbers.

The objective of this paper is the quantification of the rate of radio occultation observational impact with increasing observation number, in both the analyses and forecasts. This work extends a preliminary investigation presented by [16], who demonstrated that removing 50 % of the GPS-RO data in the Météo-France NWP system degraded the analysis and forecast quality. However, the GPS-RO measurements have been used more conservatively in their system than we do here. The present study aims at supporting current constellation assessment and future mission planning, for example in the framework of the joint University Corporation for Atmospheric Research (UCAR) - Taiwanese project COSMIC-2, the EUMETSAT Polar System Second Generation (EPS-SG), or considerations to add GNSS receivers on research missions of opportunity or commercial programmes [21].

The impact quantification is based on Observing System Experiments (OSEs) within the ECMWF data assimilation framework and by varying the number of assimilated GPS-RO observations. Section 1 describes which OSEs have been performed employing increasing numbers of observations from both operational (COSMIC, GRAS) and experimental missions (CHAMP, GRACE-A, Terrasar-X, etc.), for the period July-September 2008, which represents the most data rich time for GNSS observations so far. Given this maximum constellation, reduced scenarios can be simulated by data denial and the incremental reduction of observation impact on analyses and forecasts can be tested. This assessment is presented in Sections 2 and 3 where the main question of whether impact saturation has been reached is also addressed.

Another aspect of this study is the importance of GNSS observations to provide anchoring points for variational bias corrections that are widely applied to satellite radiances. These represent the bulk of the observational data volume in operational NWP systems. The presence of model biases, particularly in the upper troposphere - lower stratosphere (UTLS) and in the stratosphere are likely to be absorbed by radiance bias corrections. Anchoring observations, such as radiosondes and GPS-RO, reduce this effect and produce a more consistent weight given to observational data [9].

The study is summarized and conclusions are drawn in Section 4. The scenarios employed in this study also provide information on future constellation design. Furthermore, the results can be used for the “calibration” of assimilation experiments with simulated GPS-RO data, designed to estimate the impact

of increasing observation numbers significantly beyond those currently available [1].

1 Configuration

1.1 Model, data assimilation

The experiments have been run with model cycle CY36R4 of the Integrated Forecasting System (IFS) that became operational at ECMWF on 09/11/2010. This choice ensured that very recent versions of model physics, data assimilation and observation treatment were incorporated in the OSEs. The experiments have been run at reduced horizontal resolution, namely with a T511 wavenumber truncation (40 km, compared to the current operational resolution of T1279, i.e. 16 km). The vertical resolution of the experiments has been kept at 91 levels with a model top level pressure of 0.01 hPa. Previous OSEs have indicated that a reduced horizontal resolution produced sufficiently accurate results due to the large-scale structure of increments produced by temperature-related observations [4].

The system has been run in the global ECMWF 4D-Var configuration that produces two analyses per day (valid at 00 and 12 UTC) with 12-hour assimilation windows, also known as delayed cut-off data assimilation (DCDA; [12]). Only one medium-range forecast has been run per day as opposed to two forecasts in the operational configuration. Despite the different data coverage in the 00 and 12 UTC window, this is not expected to have affected the results and it provides sufficient statistical significance due to large enough samples. The main experimentation periods were chosen to be July-September 2008, the latter having been chosen because of the additional experimental GPS-RO data available for this period.

All experiments have been initialized with the operational suite on the first day of the period. A 14-day spin-up phase was included allowing for the system to adjust to the enhanced GPS-RO observing system that was activated on day one. Given that the global observation influence of the observations is about 0.2 in the ECMWF system [6], it is expected that by the end of the spin-up period, the system has lost memory of the operational system used to initialize the first analysis. The experiment evaluation has been restricted to the remaining part of the period. The evaluation has been performed based on standard observation consistency statistics and standard forecast skill scores for key parameters (geopotential heights, temperatures, vector wind at 1000, 500, 200 hPa; global and regional) including tests of statistical significance. Additional evaluation has been performed using the diagnostic tools of analysis sensitivity to observations [6].

The variational bias-correction [8, 3] for the experimentation period was initialized with the operational system output on the initial date and kept active throughout the experimentation periods. This ensured that, as in the operational system, a trade-off between analysis and bias increments as a function of model state is performed.

1.2 Background observing system

Since the experiments are meant to represent current and near-future conditions, the background that is the non-GPS-RO observing system, should mimic a configuration that will be available during the next ten years. The set of satellite sounding instruments that has been available over the past 5 years has been rather comfortable since many early satellites such as NOAA-15 are still operational but more recent systems such as the NASA-NOAA Suomi National Polar-orbiting partnership (NPP) and EUMETSAT

Table 1: Satellite radiance observing system used at ECMWF (status March 2009, monitored instruments in italic>. Comments: ¹ unstable, ² except channels 6, 11, 14, ³ insufficient data quality, ⁴ except channels 5-7, 8, ⁵ instrument failed, ⁶ except channel 7, ⁷ except channel 3, ⁸ except channels 1-4, 11-12).

Sounders	HIRS	AMSU-A	AMSU-B/MHS	Advanced Sounders
NOAA-15 (am)	No ¹	Yes ²	No ³	N/A
NOAA-16 (pm)	No ¹	Yes ⁴	Yes	N/A
NOAA-17 (am)	Yes	No ⁵	Yes	N/A
NOAA-18 (pm)	No ¹	Yes	Yes	N/A
NOAA-19 (pm)	<i>Yes</i>	<i>Yes</i>	<i>Yes</i>	N/A
AQUA (pm)	N/A	Yes ⁶	N/A	Yes (AIRS)
METOP-A (am)	Yes	Yes ⁶	Yes	Yes (IASI)

Imagers	SSM/I	SSMIS	AMSR-E	TMI	Windsat
DMSP F-13 (am)	Yes	N/A	N/A	N/A	N/A
DMSP F-14 (am)	No ⁵	N/A	N/A	N/A	N/A
DMSP F-15 (am)	Yes ⁷	N/A	N/A	N/A	N/A
DMSP F-16 (am)	N/A	<i>Yes</i>	N/A	N/A	N/A
DMSP F-17 (am)	N/A	<i>Yes</i>	N/A	N/A	N/A
AQUA (pm)	N/A	N/A	Yes ⁸	N/A	N/A
TRMM	N/A	N/A	N/A	<i>Yes</i>	N/A
Coriolis (am)	N/A	N/A	N/A	N/A	<i>Yes</i>

Metop-A/B have been added. For reference, the 2009 radiance observing system is compiled in Table 1. In addition to radiances, Clear-Sky Radiance (CSR) and Atmospheric Motion Vector (AMV) products are assimilated from Meteosat-7, 9, GOES-11, 12 and MTSAT-1R as well as AMVs from Aqua and Terra MODIS, GPS-RO observations from COSMIC 1-6 and METOP-A GRAS as well as scatterometer wind vectors from Metop-A ASCAT, the ERS-2 scatterometer and Quikscat SeaWinds, total column ozone products from NOAA-17 and 18 SBUV, Aura OMI while METOP-A GOME-2, Envisat SCIAMACHY, MSG SEVIRI, Envisat GOMOS/MIPAS data is only monitored.

Over the next 10 years, we expect to have fewer observations available since several aging satellites are expected to become decommissioned. A realistic estimate of availability is: 1 sounder system (HIRS, AMSU-A, MHS, IASI) onboard the prime Metop satellite in the mid-morning orbit, 2 conventional sounder systems (HIRS, AMSU-A, MHS) and 1 advanced sounder (CrIS) from NOAA satellites (NOAA-19, NPP, JPSS-1) in the afternoon orbit, 2 microwave imaging systems in morning orbits (DMSP F-17 or 18 SSMIS and future Department of Defense satellites), 2 scatterometers onboard Metop and Oceansat-2 (and follow-on), 3-5 GPS receivers (COSMIC, COSMIC-2, GRAS) and 3 total column ozone sensing instruments (SBUV onboard NOAA-18 or 19, GOME-2 onboard METOP and OMPS onboard NPP, JPSS-1). This set is expected to be complemented by at least five satellites in geosynchronous orbits (2 European, 2 US and 1 Japanese satellite), and altimetry data from research satellites. The number of HIRS instruments may be revised given the fact that this series will be discontinued in the future since its observing capabilities are fully covered by advanced sounders. Chinese instruments are not accounted for in this context because the expected observation quality and data availability is not sufficiently known.

In this study, the reference observing system has been defined as a subset of the operationally used set of observations described before. With respect to the operational satellite observation usage (Tab.1) the

following systems remained:

- for conventional (HIRS, AMSU-A/B, MHS) and advanced (AIRS, IASI) soundings only those from NOAA-18, AQUA and Metop-A;
- for microwave imager radiances only SSM/I data from DMSP-13;
- for total column ozone products only those from SBUV instruments on board NOAA-17 and NOAA-18;
- for scatterometry only ERS-2, QuikSCAT and Metop ASCAT data;
- only AMVs from geostationary satellites (GOES-East/West, Meteosat-7/9, MTSAT-1).

This forms the background observing system to which different GPS-RO constellations have been added.

1.3 GPS-RO constellation

The experiments with GPS-RO data have been performed for 3 months, namely July-September 2008, a period for which experimental GPS-RO data from CHAMP, GRACE-A, Terrasar-X and SAC-C have been acquired in addition to the COSMIC and GRAS data that are operationally used at ECMWF. The COSMIC data used in this study was a reprocessed dataset, using the latest operational processing code employed at the UCAR. The reprocessed COSMIC data is thus more consistent with GRAS data, in terms of bias characteristics of the bending angles in the lower/mid stratosphere, although the biases with respect to ECMWF short-range forecasts have increased. The SAC-C and Terrasar-X datasets were also processed at UCAR using the latest operational code, specifically for this study. The combined number of bending angle profiles available per day, averaged over the 3 month period, is 2940 which is about 20% more data than used in the 2009 operational system. This number is comparable to the number of occultations that are currently available (as of January 2013), since the successful launch of Metop-B on September 17, 2012, which includes one GRAS instrument.

In the control experiment all available GPS-RO data have been assimilated and three denial experiments have been run assimilating only 5, 33 and 67% of the GPSRO data, respectively. The 5% experiment (i.e. about 150 profiles) is representative of the data numbers from a single instrument like a mission of opportunity (e.g. CHAMP). The 33% and 67% experiments roughly represent a half and a full COSMIC constellation, respectively. The total number of different bending angle observations in a randomly chosen 4D-Var cycle can be seen in Table 2 and the horizontal distribution of all the assimilated GPSRO data in the same cycle is shown in Figure 1.

2 Analysis impact

Since GPS-RO observations mainly constrain temperature in the analysis with excellent vertical resolution across the mid-upper troposphere and throughout the stratosphere it is worth showing the mean ECMWF model errors as zonal cross-section (Figure 2). The mean errors are defined as the mean difference between 24-hour forecasts and operational analyses verifying at the same time. Fig.2a suggests that across the stratosphere the model has a cold bias of up to 0.5 K that broadens in altitude towards the summer hemisphere and that breaks up and becomes less pronounced towards the winter hemisphere.

Table 2: Total number of GPS-RO bending angle observations from different receivers for a given 12-hour 4D-Var assimilation window.

Type	Number	Type	Number
COSMIC-1	48,804	CHAMP	13,88
COSMIC-2	58,064	GRACE-A	11,059
COSMIC-3	44,606	Terrasar-X	22,154
COSMIC-4	59,295	SAC-C	16,714
COSMIC-5	40,596	GRAS	50,087
COSMIC-6	53,075		

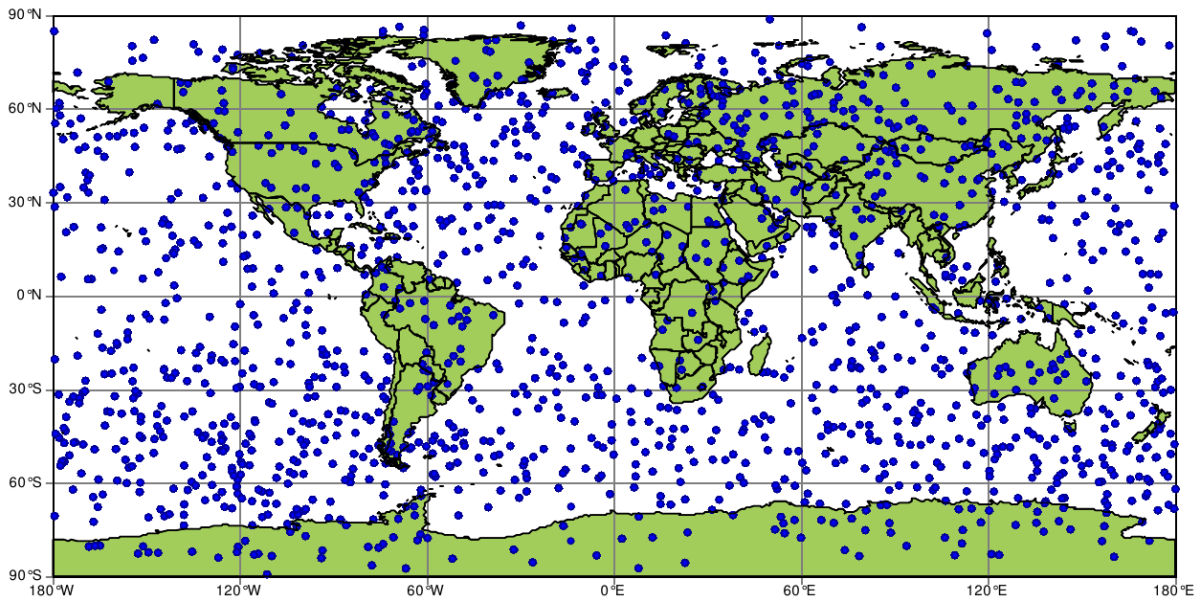
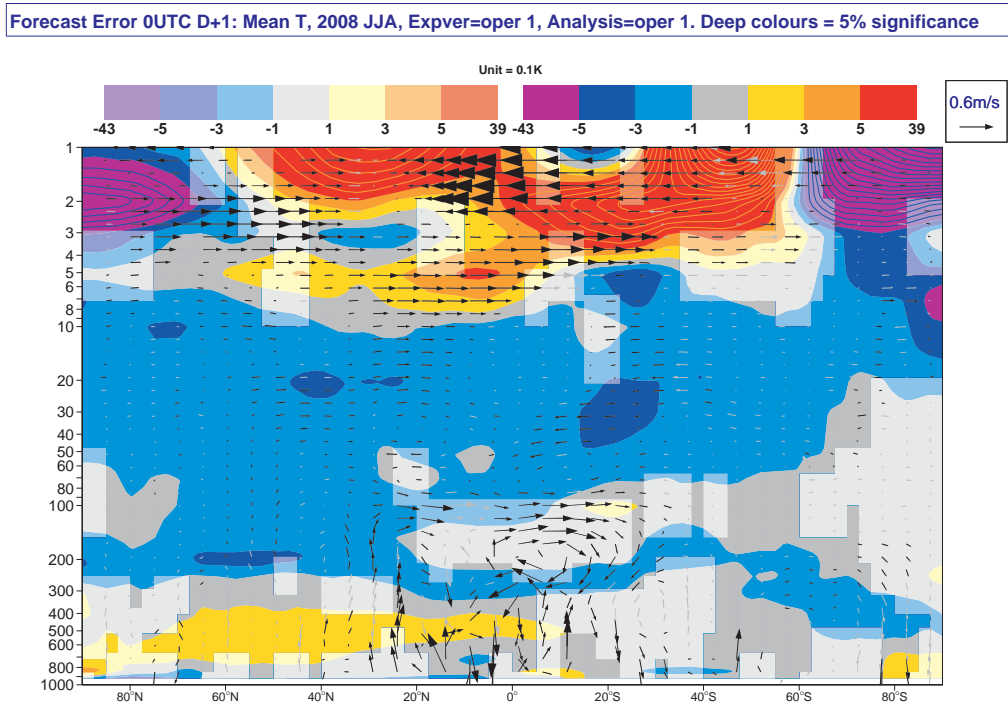


Figure 1: Horizontal distribution of all assimilated GPS-RO data for a given 12-hour 4D-Var assimilation window.

a)



b)

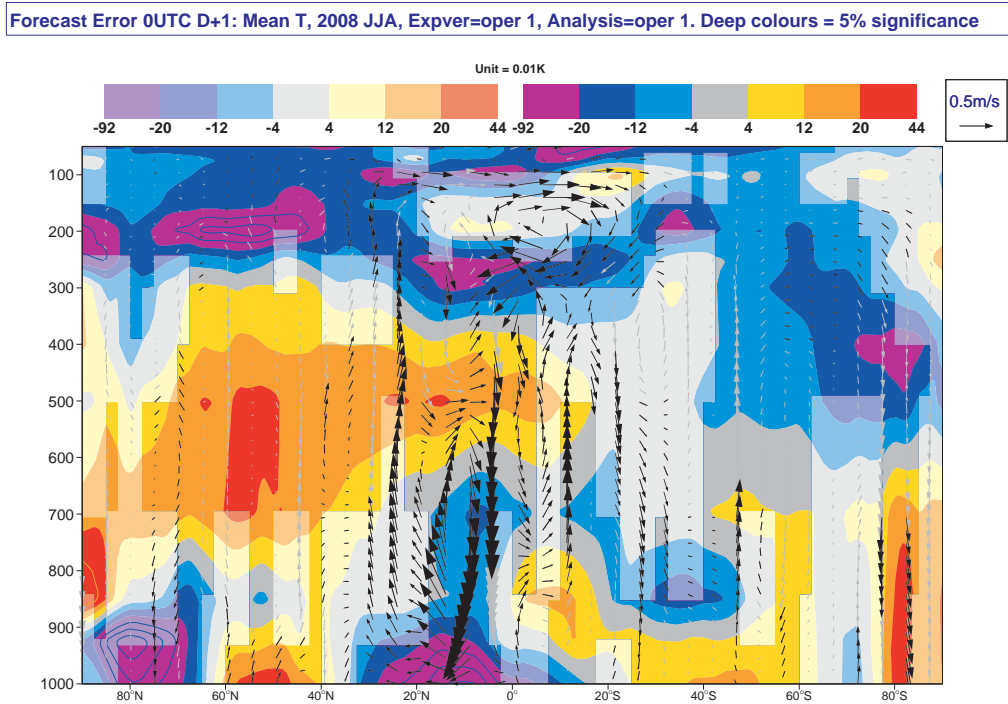


Figure 2: Mean June-July-August 2008 day-1 model temperature and meridional wind error in logarithmic (a) and linear (b) scale to emphasize stratosphere and troposphere, respectively. Bold colours indicate errors that are statistically significant.

Below the tropopause and mostly in the summer hemisphere, the bias changes sign with similar magnitude and extends down to 700-800 hPa. The positive bias is colocated with areas of summer-time convection over land and deep convection over warm oceans and the ITCZ. The cold bias in the lower stratosphere is also most pronounced in areas with convection. These structures suggest that the biases have a dependence on radiation and its interaction with water vapour, trace gases and clouds as well as on the troposphere-stratosphere exchange and the model's representation of the tropopause.

The meridional wind errors in Fig. 2 are largest in the Tropics and suggest that the Hadley circulation is generally too weak. However, the model exhibits quite substantial regional variability of lower-level divergence errors [5] depending on ocean basin and land-sea distribution. The above day-1 forecast errors tend to amplify with forecast range, particularly in the stratosphere. Thus observations systematically correct for a systematic model error in the analysis and both GPS-RO and infrared/microwave radiance data contribute most strongly to this correction in upper troposphere and stratosphere.

2.1 Mean state

Fig. 3 shows the impact of successively removing GPS-RO observations on mean temperature analysis at 100 and 200 hPa, i.e. the height region in which the mean model-minus-observation difference changes sign in the UTLS (see Fig. 6 and 7). The differences have been calculated with reference to the full constellation that is 100% of GPS-RO data being available. The sign change between these heights is clearly visible and the decreasing relative impact of GPS-RO data going towards larger observation volumes. The strongest effect is seen in the Tropics and over oceans where fewer radiosonde (and aircraft) observations are available. Therefore the weakest impact is seen over Northern mid-latitude continents where the highest density radiosonde networks are found. The GPS-RO data impact there is nearly zero and thus does not much depend on the number of available occultations. However, over oceanic areas the difference between analysis from the 67% and 100% GPS-RO coverage experiments is rather significant and suggests that even more observations will produce also stronger impact.

If the same set of experiments is run and also radiosonde data is withdrawn (Fig. 4) the main, above described features are still visible and the areas of impact are deepened. At 100 hPa the overall effect of GPS-RO data on the analysis is now even larger and now also noticeable over mid-latitude land areas in the Northern hemisphere. The impact at 200 hPa is quite similar to the experiments in which radiosonde data is included, most probably reflecting the importance of aircraft temperature measurements at this level in the Northern hemisphere. It is evident that radiosonde data, similar to GPS-RO, performs similar work on adjusting the model bias in the analysis in terms of magnitude and sign. Due to the approximately homogeneous coverage of occultations over the globe, the mean analysis increments are distributed more evenly in space (and time) and will thus produce a geographically more balanced analysis state that was not available before.

2.2 DFS

The analysis impact of individual observation types can be further illustrated using the Degree of Freedom of Signal (DFS) [6]. The DFS measures the observational influence in the data assimilation scheme as a function of data volume, observation and background error variances as well as the linearized observation/model operator. The value of mean DFS or (mean observation influence) is expected to be between 0 and 1, where mean DFS=0 means that the observation has no influence and DFS=1 means that the analysis at the given point is fully driven by that observation and not the model background. For gaining computational efficiency, the actual calculation is performed by a numerical approximation

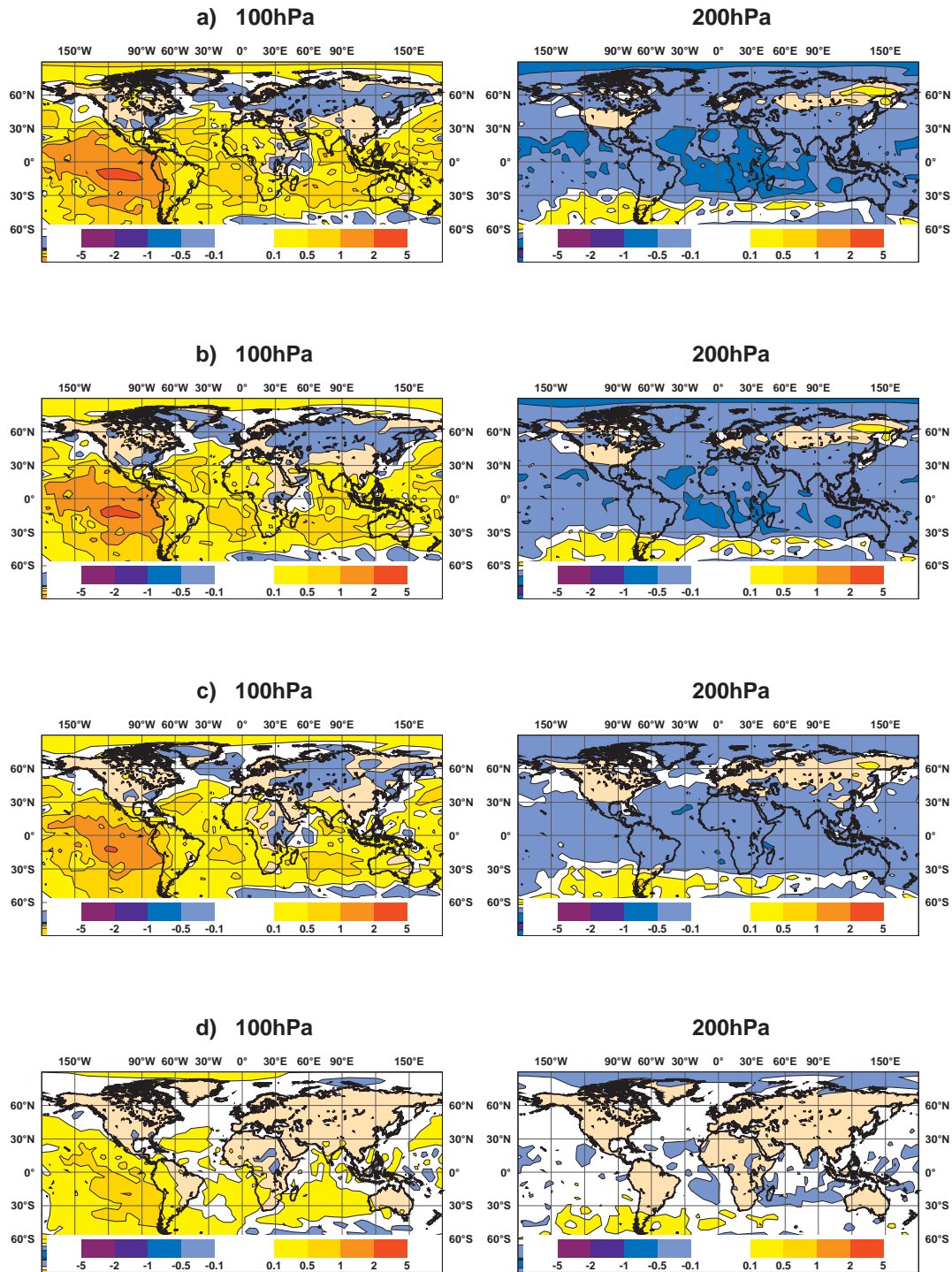


Figure 3: Mean temperature analysis difference between experiments with 100% and 67% (a), 33% (b), 5% (c) and 0% (d) of the total observation number available in July 2008. Left panels are for 100 hPa, right panels for 200 hPa level, respectively. Results from the 12 UTC analyses only.

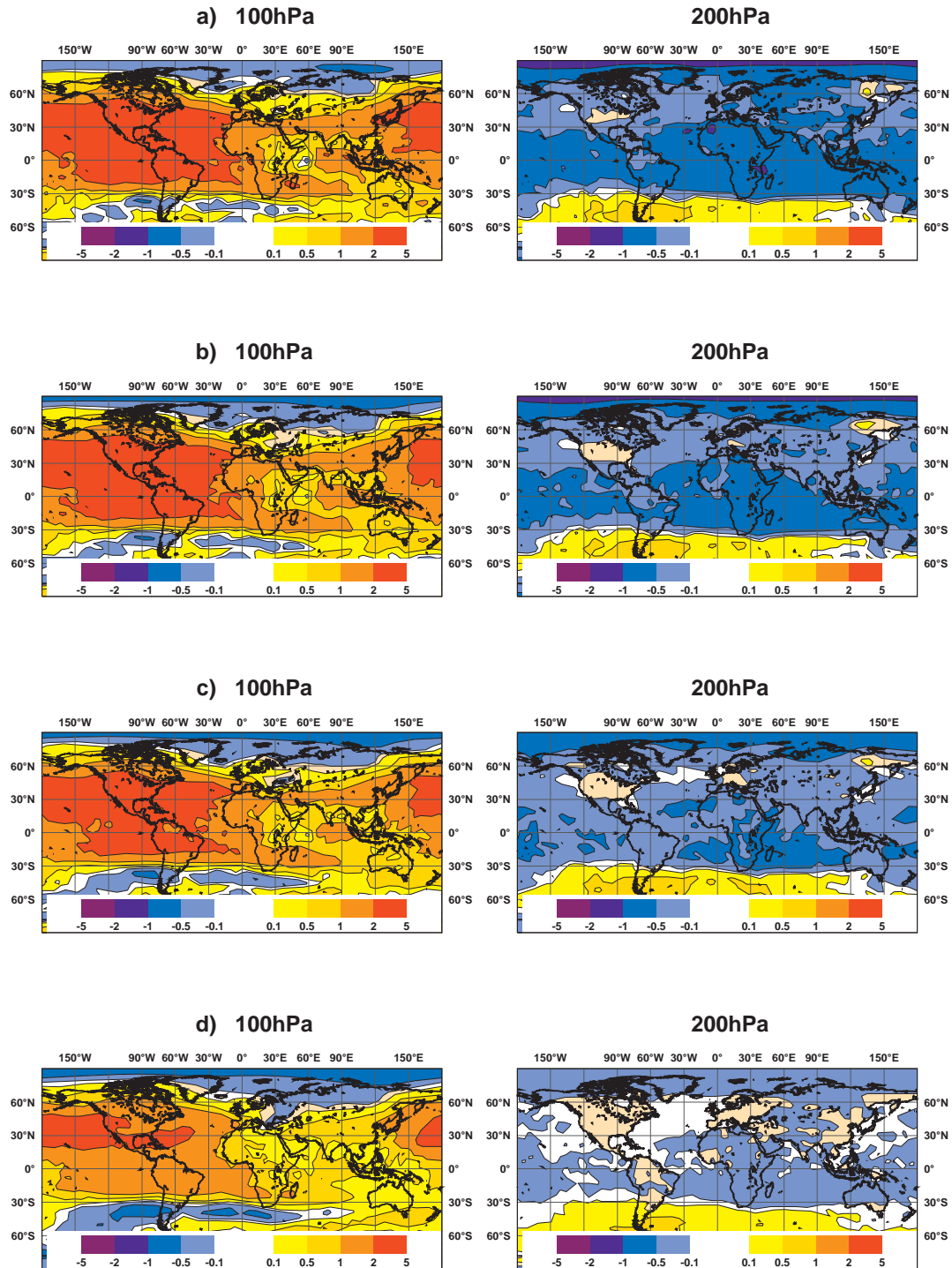


Figure 4: As Fig. 3 for experiments without radiosondes.

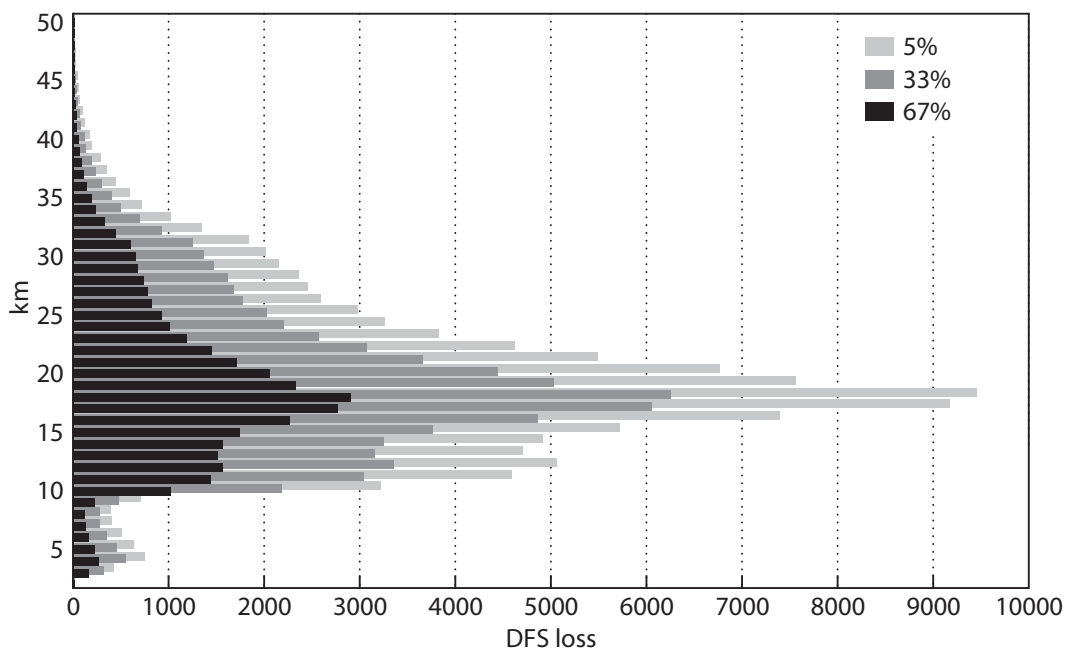


Figure 5: Vertical profile of global GPS-RO observations on DFS-loss when only 67% (black bars), 33% (dark grey bars) and 5% (light grey bars) of the data are present compared to the full constellation (100% = Ctrl). Results obtained from 16 August 2008. Units are bits.

so that values outside this range can occur. Of importance is that the DFS provides an analysis impact assessment without the need for performing OSEs and with the entire observing system being present.

The loss of total DFS as a function of GPS-RO data denial for both GPS-RO and all observations with respect to the full constellation (100% data) increases linearly with data loss to about 15% when all GPS-RO data have been withdrawn. This number emphasizes the fundamental importance of occultation measurements in the analysis given the fact that about 10 times more radiance observations are assimilated. The DFS loss can also be displayed as a function of height [?] and is largest where the mean observation influence is largest. This is shown as the vertical loss profile of DFS for the 67%, 33% and 5% OSEs in Figure 5. The figure suggests that the loss of information follows the mean observation influence profile and that it changes linearly with data volume. The total loss of information is therefore largest where the information provided by this observation type is largest, namely between 15 and 25 km, i.e. also where the largest impact of GPS-RO data on mean analysis state is seen, where the model errors change sign and the high vertical resolution of GPS-RO data is thus most beneficial.

2.3 Fit analysis-observations

Better analyses are expected to produce a consistently better fit of the model fields when compared against all observations. This assumption applies to both the analysis and first-guess, i.e. the short-range forecast that produces a first estimate of the actual state and that has been initialized from the previous analysis. This method is very stable and generally considered unambiguous.

Fig. 6 shows the fit of short-range temperature forecasts with respect to tropical radiosonde observations from the experiments using 0, 5, 33, 67, and 100% of the GPS-RO observations as listed in Tab. 2,

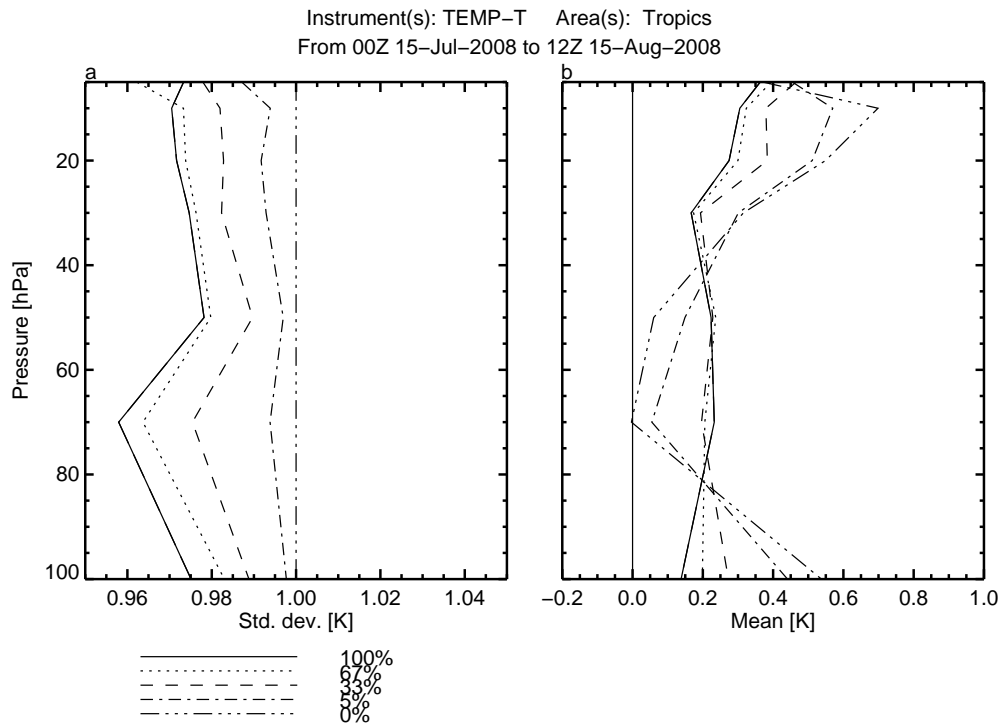


Figure 6: Departure between 9-hour model forecast (first-guess) and radiosonde observations of temperatures in the tropical stratosphere (10-100 hPa). Standard deviations (a) and biases (b) for GPS-RO OSEs with 100% (dash-triple dotted), 67% (dash-dotted), 33% (dashed), 5% (dotted) and 0% (solid) of the total observation number available in 15 July - 15 August 2008.

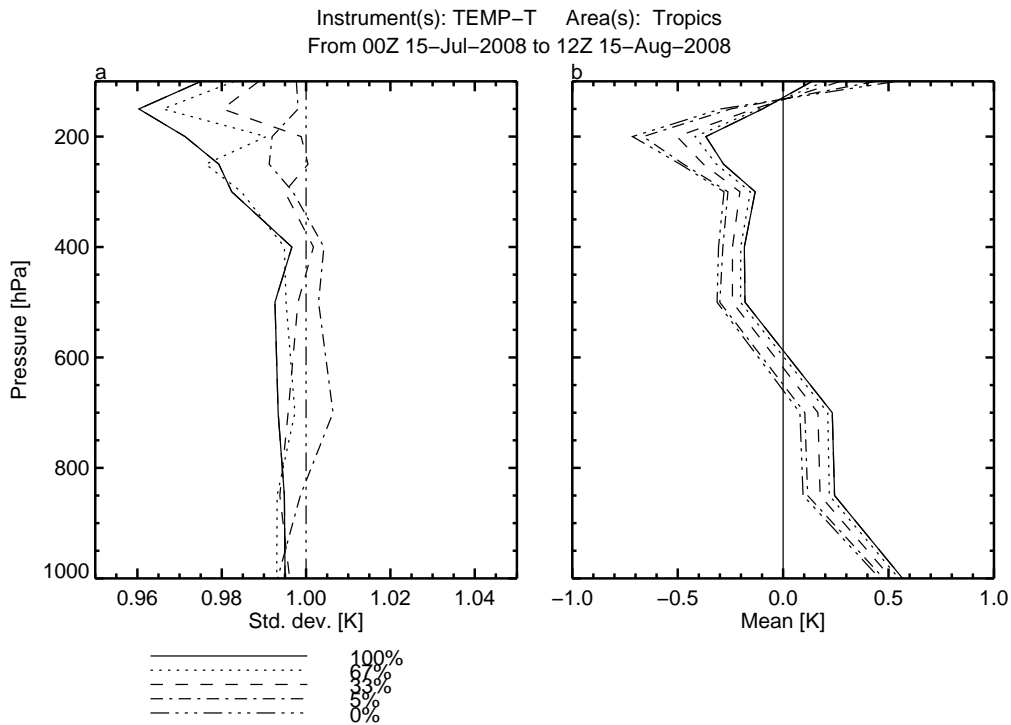


Figure 7: As Fig. 6 for troposphere (b; 100-1000 hPa).

respectively. The effect of changing GPS-RO constellation on standard deviations is shown relative to the full constellation (i.e. 100% data; Fig. 6a). Withdrawing all GPS-RO bending angles increases standard deviations by 3-4% and this change is fairly uniform between 10 and 100 hPa. Even reducing the number to 67%, i.e. reducing the maximum possible constellation to what is operationally available today, is noticeable and decreases the fits by 0.7%. The impact on biases is shown in Fig. 6b and reveals a much larger height dependence. The short-range forecast errors without GPS-RO observations are near zero between 50 and 70 hPa and increase significantly above and below this layer. Adding GPS-RO observations reduces this height dependence until a fairly constant mean difference of 0.2-0.3K is reached with the full constellation.

Between 50 and 70 hPa in the tropics, differences between the model and radiosondes in the absence of GPS-RO observations tend to be very small. This feature is also visible in Fig. 2a near 25N latitude and is the result of compensating positive errors over Northern Africa and negative errors elsewhere at this latitude and thus not an expression of generally small errors. Adding GPS-RO observations therefore reduces regional differences and produces model-observation departures that are more homogeneous across latitudes and height.

In the troposphere, the interpretation of the GPS-RO impact becomes slightly more complicated (Fig. 7). Again, the standard deviations are reduced with increasing observation number in the mid to upper troposphere. At lower levels, the impact is rather neutral and the 67% constellation even produces a slightly better fit between the model and radiosondes below 700 hPa. The mean differences show that the GPS-RO observations basically make the model colder throughout the troposphere. This cooling counteracts the model's warm bias in the upper troposphere but increases the model's warm bias in the lower troposphere. This is interpreted as an integrated effect of these observations on the atmospheric column from altitudes where the bending angles produce very large increments at levels where the model bias switches sign from the upper troposphere / lower stratosphere. The increments propagate downwards since the weighting function of the bending angle operator has a long hydrostatic tail towards the surface [10], because the computed bending angles are sensitive to the height of the model levels. This effect also has a regional pattern depending on the presence of other assimilated temperature observations as from radiosondes and aircrafts.

2.4 Bias correction anchoring

The analysis system employs a variational bias correction [8] that is applied to the majority of satellite data and selected conventional observations. This bias correction accounts for fluctuations in instrument calibration and enhances the consistency between the rather diverse observation types, but it is also prone to absorb model bias. It is therefore useful to investigate the change of bias corrections with respect to changes in the number of observations that do not require bias correction when assimilated.

Figure 8a shows the difference between the fit of the analysis to AMSU-A channel 5-14 radiance observations between experiments and the mean bias corrections applied to these observations in the Southern hemisphere (Fig. 8b). The impact of changing GPS-RO observation number on the standard deviations is visible as was the case for radiosondes but with values of 1-2% or $O(0.01 \text{ K})$ is not significant. The impact on mean differences is nearly zero but the impact on mean bias correction is more obvious (up to 0.15 K; Fig. 8b). This demonstrates that the GPS-RO observations anchor the bias correction without affecting the analysis and first-guess statistics much. The degree of anchoring changes with the number of GPS-RO observations. Bias corrections become smaller with increasing numbers for channels 6-12. This is a good sign as adding unbiased anchoring GPS-RO observations should reduce the biases across a consistent analysis system and therefore less model bias correction work is performed by the radiance

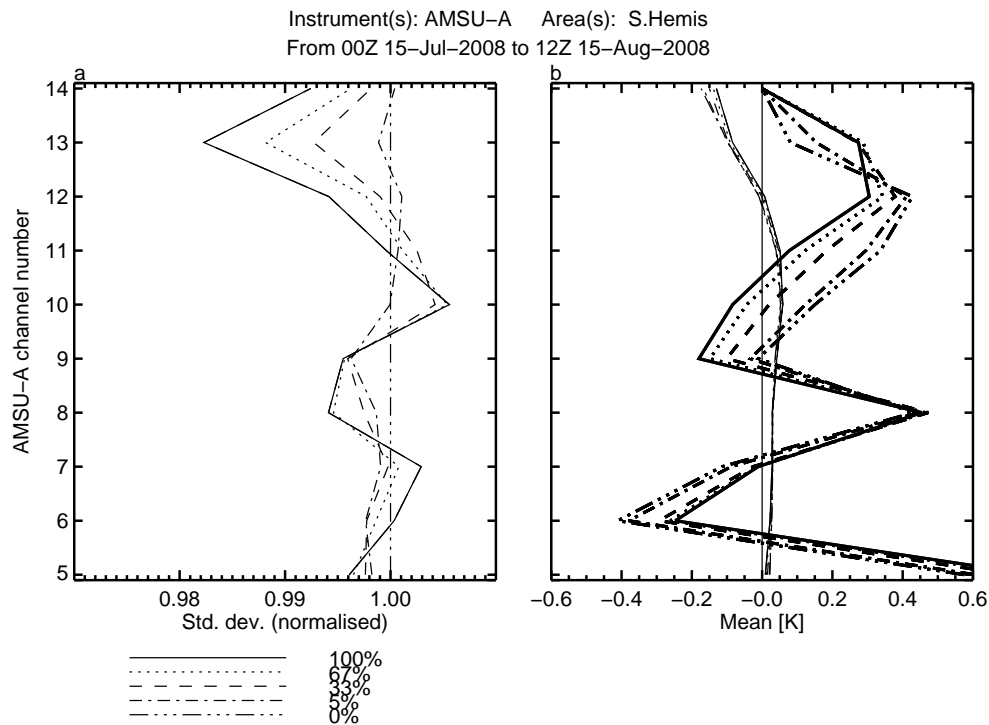


Figure 8: Model fit to AMSU-A channels 5-14 radiance observations in Southern hemisphere. Standard deviations of first-guess departures normalized to 0% GPS-RO constellation (a), mean first-guess departures (thin lines) bias corrections (thick lines) (b).

bias corrections.

The weighting functions of AMSU-A channels 6-12 peak between 400 and 10 hPa and covering those altitudes at which GPS-RO observation error variances are the smallest and therefore their effect on the analysis the strongest. Note that the weighting functions of radiance observations are fairly broad and do not resolve the more detailed model bias structure seen in Fig. 2. Thus the change of sign for bias corrections as a function of channel reflects the combined effect of model, radiometer calibration and radiative transfer biases.

As with the radiosonde temperatures (Fig. 7), the increasing bias corrections with increasing GPS-RO data volume for levels below 400 hPa (AMSU-A channel 5) relates to the downward propagation of GPS-RO temperature increments due to their long hydrostatic weighting function tail. Again, the different curves are just laterally displaced. Above 10 hPa a different mechanism comes into play. The bias correction of AMSU-A channel 14 is fixed to zero to avoid it being too strongly determined by significant model biases. This also has an impact on the bias correction of channels 12-13 due to their overlapping weighting functions. It was only possible to fix the channel 14 bias correction to zero when GPS-RO measurements were also being assimilated (A.P. McNally, pers. comm.).

Removing alternative temperature observations from the background observing system should change the above statistics in a similar way as shown in Fig. 7. Figure 9 shows this effect based on the 33% GPS-RO constellation for the Northern hemisphere where the highest density of complementary temperature observations exists. Removing radiosonde (solid) or aircraft (dotted) temperature data increases first-guess error standard deviations by a small amount and slightly increases AMSU-A bias corrections, most significantly for tropospheric channels. Again, for altitudes where GPS-RO observations receive

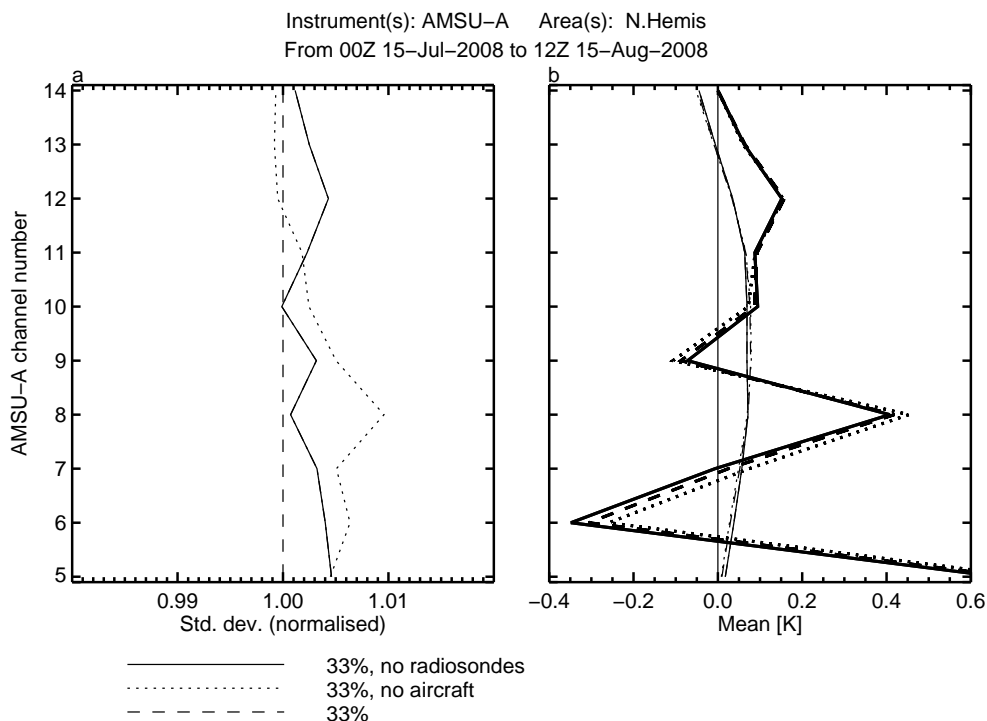


Figure 9: As Fig. 8 for Northern hemisphere. 67% GPS-RO constellation (dashed), if aircraft (dotted) or radiosonde (solid) temperature data are removed.

the highest weight (see Fig. 5), the withdrawal of data denial is least visible indicating the dominant anchoring effect by GPS-RO data. Even at levels where the assimilation of aircraft observations is most effective, e.g. at 200–250 hPa over the North Atlantic and Pacific, little impact of this data on both infrared and microwave sounder bias corrections is found. These results represent large-scale statistics and a more detailed investigation into the impact of bias correction anchoring by conventional observations on smaller spatial and temporal scales is required.

3 Forecast impact

Forecast evaluation is more difficult because different reference standards can produce rather different scores. [4] have shown that an evaluation with the experiment's own analysis or the operational analysis can produce inconsistent results, in some cases with opposite signs. The argument for using the experiment's own analyses for evaluation is that if an additional observation is expected to change the mean analysis state, only the own analysis provides a fair reference while any other would produce a poorer analysis state. This, however, can also produce problems in case of a sub-optimal observing system and simply due to the fact that additional observations can add systematically larger increments to the analysis and therefore increase the root-mean-square difference between (short-range) forecasts and analyses.

Standard forecast evaluation in this study is performed with the operational analyses. The operational observing system contains more data in the above experimentation periods since the background system of the experiments was designed to represent conditions expected in the forthcoming ten years. Addi-

tionally, the operational system is run at higher spatial resolution.

Figure 10 shows the normalized RMS forecast error difference between the different GPS-RO denial experiments (0-67%) and the control experiment (100%) for tropospheric temperatures. Down to 500 hPa the more GPS-RO data is used the better the scores become. The impact lasts 2-3 days at 200 hPa and 700 hPa but into the medium range at 500 hPa. The error reduction at 200 hPa is rather dramatic and reaches 50% at day-1 in the Tropics and Southern hemisphere.

The negative effect of adding GPS-RO observations at 1000 hPa, especially in the Tropics, matches the radiosonde statistics in Fig. 7. The GPS-RO data produces a cooling in the mid-to-upper troposphere that propagates down towards the surface where the data loses vertical resolution. There, it is also affected by increased noise but is assimilated with increased observation error variances. The model bias switch of sign from a cold to a warm bias in the boundary layer which the GPS-RO observations are not able to resolve. Therefore the dominant upper atmospheric signal tropospheric pushes the analysis away from other observations and thus increases the analysis and forecast errors near the surface.

Another feature in Fig. 10 is a negative impact between days 2 and 4 at 200 hPa in the Northern hemisphere and at 500 hPa in the Southern hemisphere. Again, this deterioration increases with GPS-RO data volume. This degradation is most likely an artefact from the differences in GPS-RO data pre-processing between the denial experiments and the operational system, the latter being used for verification in this figure. The UCAR-processing (see Section 1.3) translates to a small but noticeable change of observation-minus-model biases that produces sub-optimal analyses. Areas where the model bias changes sign are particularly sensitive to this difference.

Figure 11 presents the reduction of temperature forecast errors across stratosphere and troposphere relative to the OSE in which all GPS-RO have been withdrawn. Note that 24-hour forecast errors are between 0.5 and 1.5 K, and that the largest errors are found near 100 hPa and in the Tropics. The relative improvement of scores by adding GPS-RO observations is significant when 5% and 33% of the totally available data is added and tapers slightly off by adding more data. Error reduction reaches more than 20% at 50, 100 and 150 hPa and becomes weaker in the mid to lower troposphere. An important observation is that - given the shape of the curves - impact saturation has not been reached and that we can expect further improvement if more data were available. Within the context of this study it was not tested whether reducing observation errors and thus increasing GPS-RO observation weight could produce such a saturation. The retuning of observation errors is rather complex and should not be performed for one observing system in isolation.

Lastly, the general capability of GPS-RO data to constrain temperature analyses has been compared with other satellite data, especially from advanced sounders. This has been investigated with another set of experiments in a poor-baseline context, in which no satellite radiance and aircraft observations have been assimilated. This set-up helps to amplify the impact of individual observing systems and thus to distinguish individual contributions from the non-linear superposition of all components in an operational framework. Here, the experiments have been again verified with the operational ECMWF analysis.

Figure 12 shows the temperature RMS forecast error reduction at various levels and latitude bands if GPS-RO (100%; red curves) or IASI radiance data (black curves) are added to the baseline, respectively. Note that these experiments reflect that typically 3 million IASI radiances and 300,000 bending angles are being assimilated per 12-hour cycle. At 200 hPa in the Southern hemisphere and at 500 hPa in the Tropics, both observing systems produce almost identical impact. At 200 hPa in the Tropics, GPS-RO data even outperform IASI data for the first 2 days. At the remaining levels and areas, IASI performs slightly better. In the Northern hemisphere, the difference between all experiments is smaller due to the large conventional observation density. While these experiments do not reflect the individual instru-

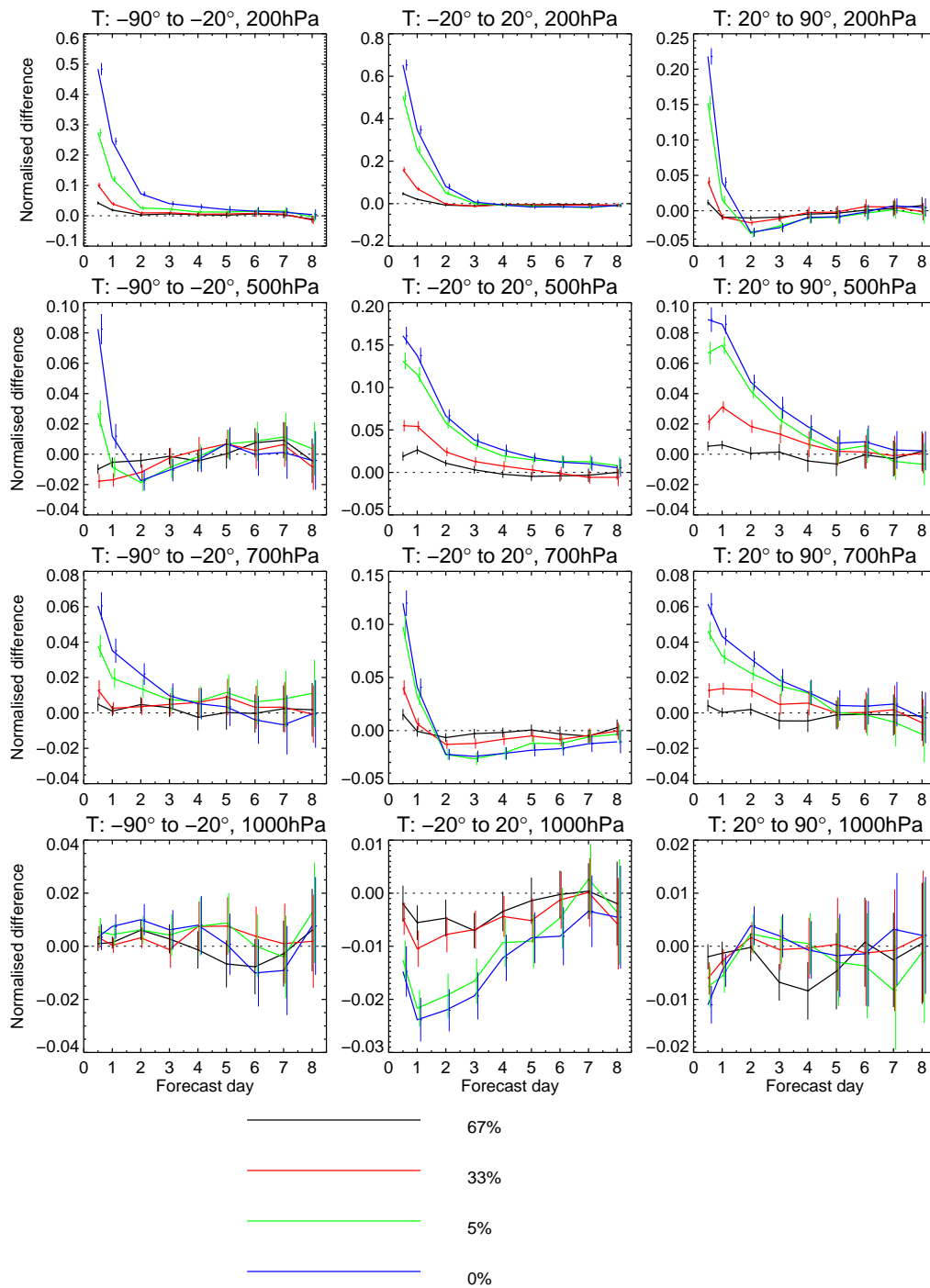


Figure 10: Normalized RMS error difference between GPSRO denial experiments (numbers denote the percentage used) and control for temperature. Positive values indicate positive impact of GPSRO data. Columns refer to Southern hemisphere, Tropics and Northern hemisphere (from left to right). Rows correspond to 200, 500, 700 and 1000 hPa (from top to bottom). Forecast verification is against operational analysis, verification period is 01/07-30/09/2008.

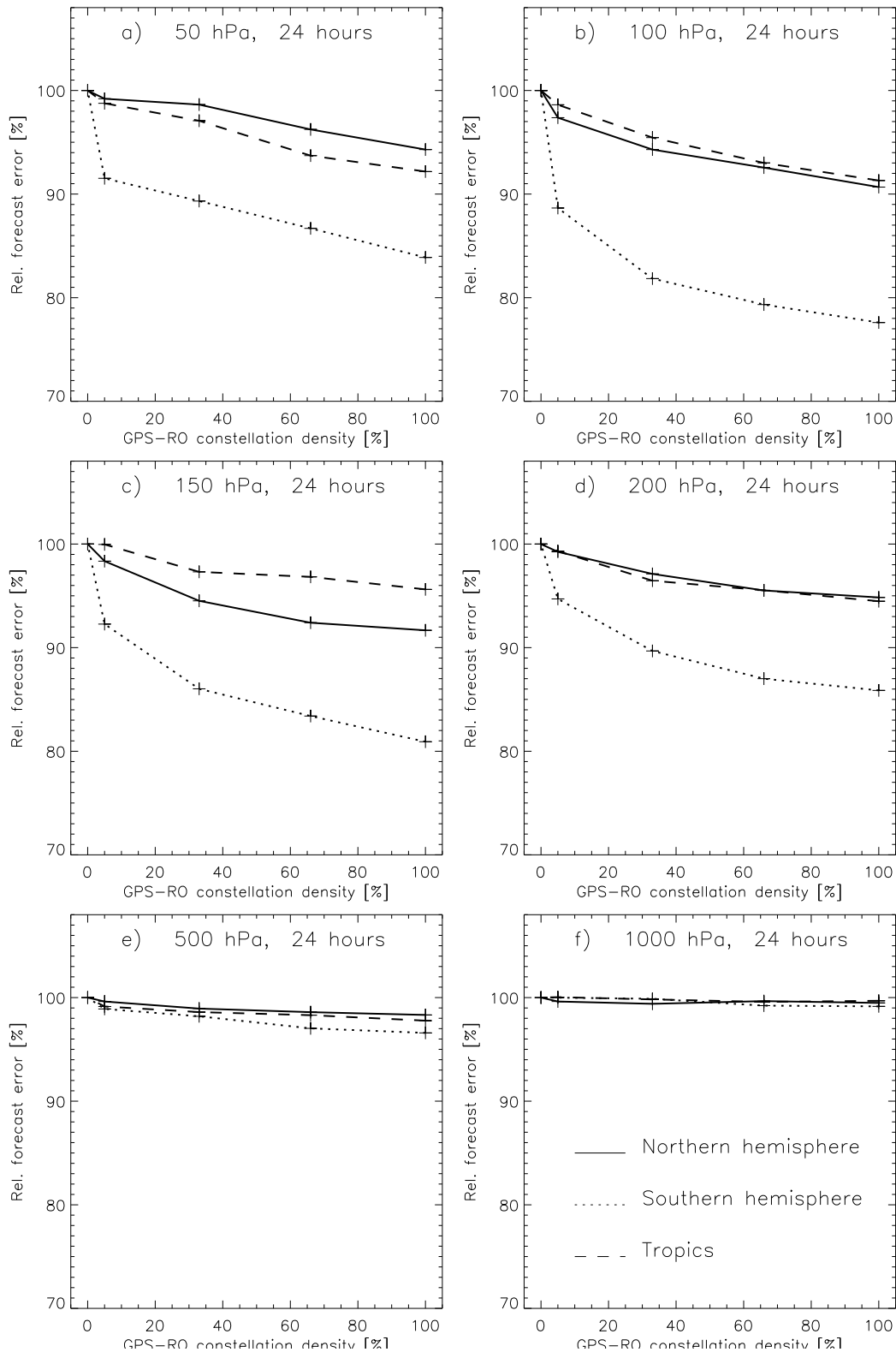


Figure 11: Dependence of 24-hour temperature forecast error relative to 0%-GPS-RO experiment (in %) at 50 (a), 100 (b), 150 (c), 200 (d), 500 (e) and 1000 (f) hPa. Solid, dotted and dashed lines denote scores for Northern, Southern hemisphere and Tropics, respectively, over period 15/07- 15/08/2008.

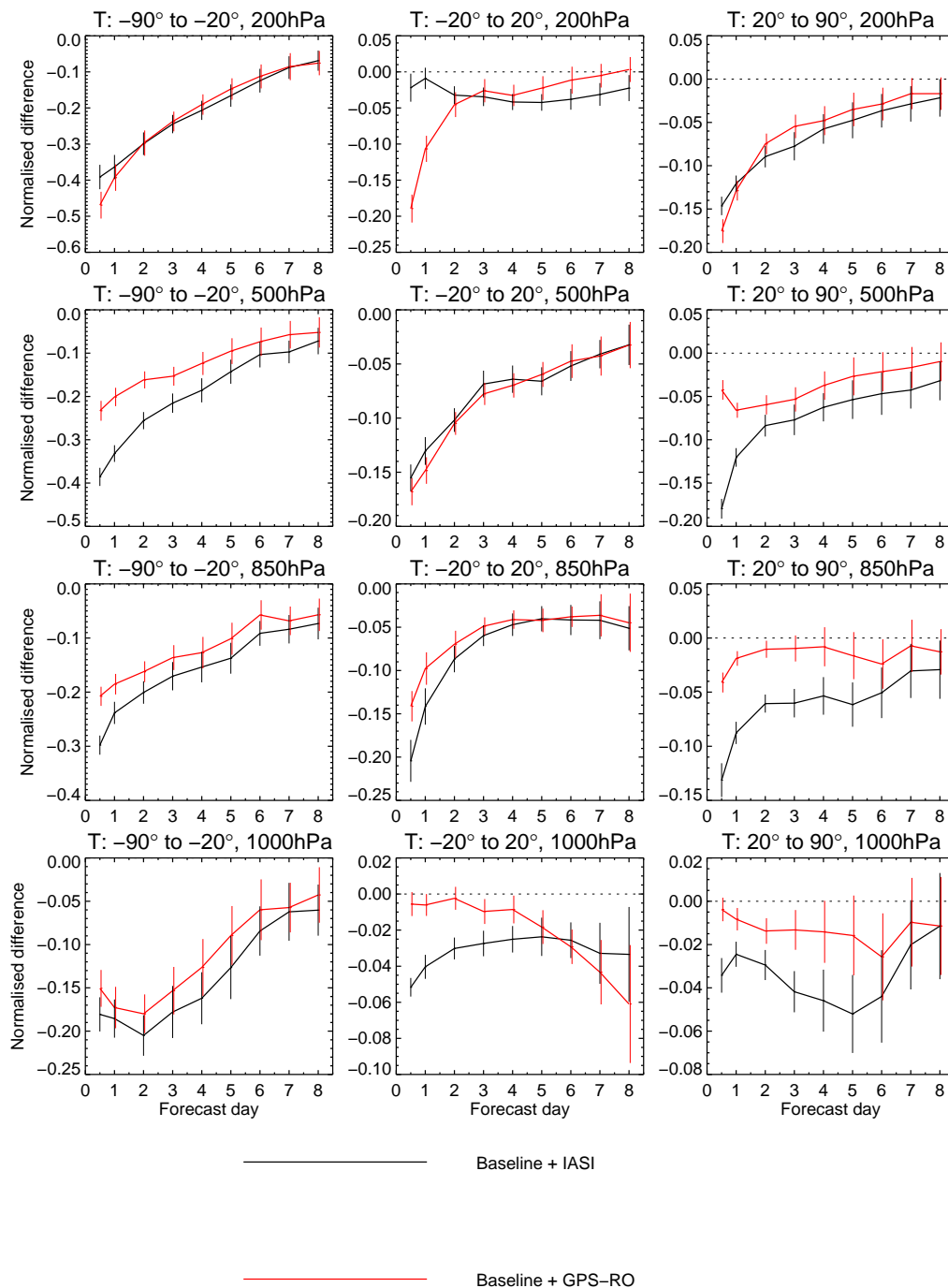


Figure 12: Temperature forecast root mean square error reduction if GPS-RO (red) or IASI (black) data is added to a baseline observing system (see text for details). Columns refer to Southern hemisphere, Tropics and Northern hemisphere (from left to right). Rows correspond to 200, 500, 850 and 1000 hPa (from top to bottom). Forecast verification is against operational aECMWF analysis, verification period is 07/07-31/08/2008.

ment impact in a fully operational framework, they highlight how powerful GPS-RO data are in current systems and how this can compare to other, rather sophisticated instruments.

4 Summary and conclusions

GPS-RO data represent a very important part of the observing system because they do not require bias correction and produce accurate observations of (mainly) temperature with very good vertical resolution in the upper atmosphere where radiance data is more sparse and NWP model errors are large. For the experiments in this study, CHAMP, GRACE-A, Terrasar-X and SAC-C data in addition to the currently assimilated receivers onboard METOP GRAS and the Formosat-COSMIC constellation have been acquired to make available as many GPS-RO observations as possible. All data have been assimilated and three denial experiments have been run using only 5, 33 and 67% of the GPS-RO data, respectively. The 5% experiment (i.e. about 150 profiles) is representative of the data numbers from a single receiving instrument while the 67% experiment corresponds to the number available from six satellite constellation like COSMIC.

The results from the 5% experiment indicate that the impact on temperature analysis is significant but not yet sufficient to remove the entire upper atmospheric temperature bias. An important aspect is that model bias changes sign across the tropopause (too warm upper troposphere, too cold lower stratosphere) and that this bias has a seasonal cycle, being more pronounced in the summer hemisphere. GPS-RO observations produce high vertical resolution but are assimilated in concert with other, lower resolution observations such as radiances (with similarly broad bias corrections), and with background error covariance structures that are not well resolved at these levels as well. Thus, the net effect of adding GPS-RO observations is filtered. This also points at areas with large potential for future impact enhancement.

Gradually increasing the number of observations further corrects the model bias and the analysis fits to radiosonde observations clearly indicate that more observations would produce even more benefit. The radiosonde fits also suggest that the impact has a vertical structure that follows the model bias, namely that GPS-RO data warm the analysis in the stratosphere and cool it in the troposphere. The impact is also affected by other observations in the system and running further experiments in which radiosonde and aircraft data have been withdrawn as well demonstrated a significant amplification of the GPS-RO contribution. Evaluating the information content of the observations reveals that the information loss increases linearly with the number of observations and follows the vertical profile of mean observation influence. This means that losing GPS-RO observations affects most strongly those heights at which the observations have the largest impact and which coincide with the levels of best vertical resolution, smallest observation error variances and yet model errors with the largest vertical gradients.

The significant role of GPS-RO observations as anchors in variational radiance bias correction schemes has been demonstrated. Bias corrections become smaller the more GPS-RO data are available. The radiance bias corrections also show sensitivity to removing radiosonde and aircraft temperature observations; however this is mostly visible in the troposphere whereas GPS-RO data dominate the anchoring throughout the stratosphere. Again, the anchoring effect scales with available data volume.

RMS temperature forecast errors and geopotential height anomaly correlations are positively affected by GPS-RO data, especially in the higher atmosphere. Above 200 hPa the impact remains visible even for 7 days. A surprising negative effect is found, however, at 1000 hPa, especially over the Tropics for temperature. This degradation is very likely due to large increments in the upper troposphere propagating downwards and simply shifting the entire profile towards lower temperatures. Since the model bias switches sign again in the lower troposphere, the increments produce enhanced errors. This is in

agreement with boundary layer radiosonde statistics from the analyses.

At higher levels the strongest forecast improvement from adding GPS-RO observation is seen in the Southern hemisphere, where fewer radiosonde and aircraft temperature observations are available than elsewhere. From the available observations, no clear saturation effect could be found. Even with 50% more observations than assimilated in today's operational systems (i.e. 100%/67%), further improvement in short-range scores is seen. The actual level of saturation can only be derived from experiments that are based on simulated observations. Given the importance of GPS-RO observations for NWP and the current decline of available satellite instruments, it is worth investigating the sensitivity of NWP analyses and forecasts to larger than existing constellations to produce recommendations for space agencies.

Finally, baseline experiments have been run to compare the impact of IASI radiance data with that of GPS-RO observations. Up to 500 hPa the IASI impact is clearly stronger. At 200 hPa over the Southern hemisphere IASI and GPS-RO seem to be of equal impact. Over the Tropics GPS-RO observations appear to bring slightly more improvement than IASI. Over the Northern hemisphere and in the first two days GPS-RO data improve the forecast slightly stronger, but afterwards the IASI impact overtakes. These results have to be viewed keeping in mind that about one order of magnitude more IASI radiances than bending angles are assimilated at ECMWF.

Acknowledgements

Gábor Radnóti was funded by EUMETSAT contract EUM/CO/09/4600000644 and EUCOS contract EUCOS-ADM-2010-001. Sean Healy is funded by the EUMETSAT Radio Occultation Meteorology Satellite Application Facility (ROM SAF). The reprocessing of the COSMIC, Terrasar-X, GRACE-A, CHAMP and SAC-C data was performed by Bill Schreiner, Doug Hunt and Sergey Sokolovskiy (UCAR) and was crucial for performing this study. This work is greatly acknowledged. The authors are grateful for the valuable comments and suggestions from Tony McNally and Florian Harnisch.

References

- [1] R. A. Anthes, P. A. Bernhardt, Y. Chen, L. Cucurull, K. F. Dymond, D. Ector, S. B. Healy, S.-P. Ho, Y.-H. Hunt, D. C. Kuo, H. Liu, C. Manning, K. and McCormick, T. K. Meehan, W. J. Randel, C. Rocken, W. S. Schreiner, S. V. Sokolovskiy, S. Syndergaard, D. C. Thompson, K. E. Trenberth, T.-K. Wee, N. L. Yen, and Z. Zeng. The COSMIC/FORMOSAT-3 Mission: Early Results. *Bull. Amer. Meteor. Soc.*, 89:313–333, 2008.
- [2] J. M. Aparicio and G. Deblonde. Impact of the assimilation of CHAMP refractivity profiles in Environment Canada global forecasts. *Mon. Wea. Rev.*, 136:257–275, 2008.
- [3] T. Auligné, A. P. McNally, and D. P. Dee. Adaptive bias correction for satellite data in a numerical weather prediction system. *Q. J. Roy. Meteorol. Soc.*, 133:631–642, 2007.
- [4] P. Bauer and G. Radnóti. Study on Observing System Experiments (OSEs) for the evaluation of degraded EPS/Post-EPS instrument scenarios. *Study report available from ECMWF, Reading, UK.*, page 99 pp., 2009.
- [5] P. Bechtold, P. Bauer, P. Berrisford, J. Bidlot, C. Cardinali, T. Haiden, M. Janousek, D. Klocke, L. Magnusson, A. McNally, F. Prates, M. Rodwell, N. Semane, and F. Vitart. Tropical errors and convection. *ECMWF Technical Memorandum.*, 685:82 pp., 2012.
- [6] C. Cardinali, S. Pezzulli, and E. Andersson. Influence-matrix diagnostic of a data assimilation system. *Q. J. Roy. Meteorol. Soc.*, 130:2767–2785, 2004.
- [7] L. Cucurull, J. C. Derber, R. Treadon, and R. J. Purser. Assimilation of Global Positioning System Radio Occultation Observations into NCEP’s Global Data Assimilation System. *Mon. Wea. Rev.*, 135:3174–3193, 2007.
- [8] D.P. Dee. Bias and data assimilation. *Q. J. Roy. Meteorol. Soc.*, 131:3323–3343, 2005.
- [9] D.P. Dee and S. Uppala. Variational bias correction of satellite radiance data in the era-interim reanalysis. *Q. J. Roy. Meteorol. Soc.*, 135:1830–1841, 2008.
- [10] J. R. Eyre. Assimilation of radio occultation measurements into a numerical weather prediction system. Technical Memorandum 199, ECMWF, Reading, UK, 1994.
- [11] F. Harnisch, S. B. Healy, and P. Bauer. Estimating the optimal number of gnss ro measurements for nwp. *Mon. Wea. Rev.*, page submitted, 2013.
- [12] J. Haseler. Early delivery suite. *ECMWF Tech. Memo.*, 454:26 pp., 2004.

- [13] S. B. Healy and J.-N. Thépaut. Assimilation experiments with CHAMP GPS radio occultation measurements. *Q. J. Roy. Meteor. Soc.*, 132:605–623, 2006.
- [14] E. R. Kursinski, G. A. Hajj, W. I. Bertiger, S. S. Leroy, T. K. Meehan, L. J. Romans, J. T. Schofield, D. J. McCleese, W. G. Melbourne, C.L. Thornton, T. P. Yunck, J. R. Eyre, and R. N. Nagatani. Initial results of radio occultation observations of earth’s atmosphere using the Global Positioning System. *Science*, 271:1107–1110, 1996.
- [15] P. Poli, S. B. Healy, and D. P. Dee. Assimilation of Global Positioning System radio occultation data in the ECMWF ERA-interim reanalysis. *Q. J. Roy. Meteor. Soc.*, 136:1972–1990. doi: 10.1002/qj.722, 2010.
- [16] P. Poli, S. B. Healy, F. Rabier, and J. Pailleux. Preliminary assessment of the scalability of gps radio occultations impact in numerical weather prediction. *Geophys. Res. Lett.*, 35:doi: 10.1029/2008GL035873, 2008.
- [17] P. Poli, P. Moll, D. Puech, F. Rabier, and S. B. Healy. Quality control, error analysis, and impact assessment of FORMOSAT-3/COSMIC in numerical weather prediction. *Terr. Atmos. Ocean*, 20:101–113, 2009.
- [18] M. P. Rennie. The impact of GPS radio occultation assimilation at the Met Office. *Q. J. Roy. Meteor. Soc.*, 136:116–131. doi: 10.1002/qj.521, 2010.
- [19] C. Rocken, R. Anthes, M. Exner, D. Hunt, S. Sokolovsky, R. Ware, M. Gorbunov, W. Schreiner, D. Feng, B. Herman, Y.-H. Kuo, and X. Zou. Analysis and validation of GPS/MET data in the neutral atmosphere. *J. Geophys. Res.*, 102:29.849–29.866, 1997.
- [20] J. Wickert, Ch. Reigber, G. Beyerle, R. König, C. Marquardt, T. Schmidt, L. Grunwaldt, R. Galas, T.K. Meehan, W.G. Melbourne, and K. Hocke. Atmosphere sounding by GPS radio occultation: First results from CHAMP. *Geophys. Res. Lett.*, 28:3263–3266, 2001.
- [21] D.L. Wu, A.J. Mannucci, F. Xie, C.O. Ao, D.J. Diner, and J.P. Teixeira. Climate and weather sensors on iridium-NEXT: a combined GPS-RO and WindCam system for PBL remote sensing. *Proc. GEOScan Workshop, Annapolis, Maryland, March 29, 2011, Jet Propulsion Laboratory, National Aeronautics and Space Administration.*, 2011.